PHYSICAL REVIEW A **84**, 062716 (2011)

# Charge transfer in collisions between diatomic molecular ions and atomic hydrogen using merged beams

V. M. Andrianarijaona,[1] I. N. Draganić,[2] D. G. Seely,[3] and C. C. Havener[2]
[1]*Department of Physics, Pacific Union College, Angwin, California 94508, USA*
[2]*Physics Division, Oak Ridge National Laboratory, Oak Ridge, Tennessee 37831, USA*
[3]*Department of Physics, Albion College, Albion, Michigan 49224, USA*
(Received 24 October 2011; published 27 December 2011; corrected 30 December 2011)

A merged-beam technique is used to measure charge transfer (CT) cross sections for the ($O_2{}^+$,D) and ($CO^+$,D) systems over a wide range of collision energy from 20 eV/u to 2 keV/u. At the higher energies where the collision is rovibrationally frozen and the differences in the $Q$ values of the CT process can be neglected, the cross sections all converge to $(7.5 \pm 0.5) \times 10^{-16}$ cm$^2$ at 2 keV/u and are consistent with a rovibrational frozen ($H_2{}^+$,H) calculation. Toward lower velocities, ($O_2{}^+$,D) and ($CO^+$,D) have consistently similar cross sections but diverge below 60 eV/u. In contrast, previously reported merged-beam measurements for ($D_2{}^+$,H), a system with fewer electrons on the molecular core, no electronic excited states, and relatively fewer charge transfer channels, shows a decreasing cross section toward lower energies. These different trends are compared to previous merged-beam measurements of charge transfer with H for several atomic 4+ ions ($Si^{4+}$, $Ne^{4+}$, $N^{4+}$, and $C^{4+}$) which have a variety of electrons on the core.

DOI: 10.1103/PhysRevA.84.062716 PACS number(s): 34.70.+e

## I. INTRODUCTION

Knowledge of charge transfer (CT) for molecular ion-neutral collisions is necessary for the modeling of high-density, low-temperature plasmas, as can be found in cold divertor regions of a fusion tokamak. Accurate cross sections of the entire spectrum of excited molecules is necessary for understanding the formation of the detachment layer desired for the reduction of heat loads on divertor plates [1]. CT with an atomic hydrogen target is of special interest because of its fundamental aspect and its importance in interstellar clouds. In the low density of the interstellar medium including dense clouds, the majority of interstellar molecules are formed by ion-neutral reactions including charge transfer processes efficient at low temperatures (UMIST database) [2].

Measurements of molecular ion charge transfer with atomic H is a particular experimental challenge. A H target can be difficult to produce and characterize, resulting in few measurements at limited collision energies. There have been ion-flow drift tube studies where the amount of atomic H was estimated by observing the $COH^+$ products from the introduction of $CO_2{}^+$. In this way, for example, the $O^+$, $CO^+$, and $CH^+$ reaction rates with H have been measured at 300 K [3]. For the fundamental system $H_2{}^+ + H$, which has been studied using a variety of detailed theoretical approaches [1,4–6], there is surprisingly little experimental measurement for comparison. Using a crossed-beam technique where a thermal energy hydrogen beam was produced using a tungsten tube furnace, McGrath *et al.* [7] performed one of the first experimental investigations on the $H_2{}^+ + H$ collision system in the energy range between 10 and 50 keV. Their results indicate that the dissociative and nondissociative CT channels dominate collision reactions toward lower energies. These measured cross sections for dissociative and nondissociative CT in $H_2{}^+ + H$ at the higher energies are also consistent but yet significantly below the sudden approximation calculations [6]. At the lower energies where the rovibrational states become important, theory becomes difficult. A fully quantal state-to-state calculation [4] has been performed for collision energies from 0.2 to 10 eV/u and extended [5] up to 100 eV/u using a semiclassical straight-line trajectory approximation for the projectile motion. Tabulated results for both calculations are available on the Oak Ridge National Laboratory's (ORNL) Controlled Fusion Atomic Data Center (CFADC) website [5]. While ORNL merged-beam measurements are now in progress for CT in $H_2{}^+ + H$ collisions, a detailed comparison has been previously made for $D_2{}^+ + H$ from 0.1 eV/u to 2 keV/u [8]. This molecular ion measurement with the merged-beam apparatus benchmarks the sudden approximation theory appropriate at the higher energies and the vibrational specific adiabatic theory for the $(H_2\text{-}H)^+$ complex at the lower energies. ORNL CT merged-beam measurements have also been reported for $D_3{}^+ + H$ from 2 eV/u to 2 keV/u [9].

In this paper, we report the measurements of the cross section for ($O_2{}^+$,D) and ($CO^+$,D) over an extended energy range from 20 eV/u to 2 keV/u using the ORNL ion-atom merged-beam apparatus and compare to our previous results for the fundamental ($D_2{}^+$,H) system [8]. Note, for the measured charge transfer reaction, e.g., ($CO^+$,D),

$$CO^+ + D \rightarrow CO^* + D^+,$$

we only measure the $D^+$ product of the reaction. Therefore our measurements do not distinguish between the dissociative and nondissociative channels of the product $CO^*$. Dissociation may occur if it is energetically possible. Ionization of D is not expected at these low collision energies.

A succinct description of the upgraded ORNL ion-atom merged-beam apparatus is given in Sec. II. In Sec. III, our measurements are compared with available theories at higher energies where the rovibrational states can be considered frozen and at lower energies where the collision times are comparable to characteristic rovibrations. Our conclusion is drawn in Sec. IV.

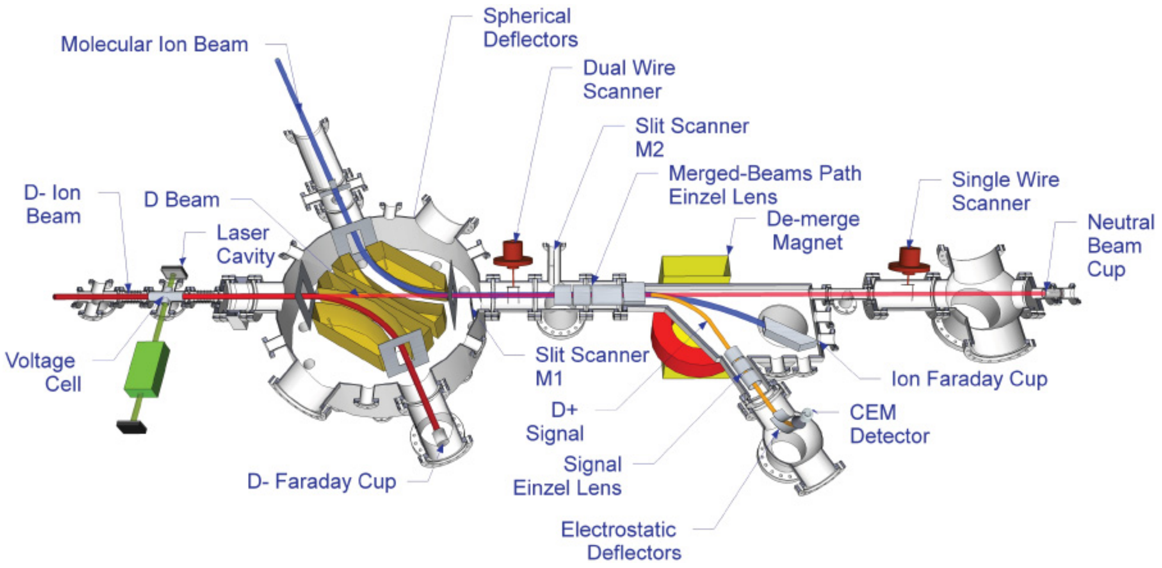

FIG. 1. (Color online) Schematic of the current ORNL ion-atom merged-beam apparatus. The merge path (32.5 cm) begins at the exit of the electrostatic spherical deflectors and ends in an Einzel lens just before the demerge magnet. A discussion of the various elements can be found in the text.

## II. DESCRIPTION OF THE EXPERIMENT

The Multicharged Ion Research Facility (MIRF) ion-atom merged-beam apparatus at ORNL has been successful for many years [10–13] in producing absolute CT cross sections for a variety of atomic ions on H and D. More recently with the development of intense molecular ion beams produced by an electron cyclotron resonance (ECR) ion source [14], the apparatus has been used for molecular ion studies [8,9]. The description of the MIRF ion-atom merged-beam apparatus upgraded to accept beams from the CEA-Grenoble all-permanent magnet ECR ion source mounted on a 250-kV high-voltage (HV) platform has been detailed elsewhere [15]. Only a brief description is given here. A schematic of the current apparatus is shown in Fig. 1. In the merged-beam technique, fast (keV) atomic or molecular ion beams are merged with H or D neutral beams, producing center-of-mass collision energies from meV/u to keV/u. The ion beam accelerated up to 150 kV from the HV platform is merged by using electrostatic spherical deflectors with a neutral ground-state H or D beam. For the $O_2^+$ and $CO^+$ measurements reported here, deuterium was used to obtain the slower velocities needed for velocity matching with the relatively heavy singly charged molecular ions. For example, for the measurements with $O_2^+ + D$, the 9.1-keV D beam is merged with a 16.7–125 keV/u $O_2^+$ beam, resulting in collisions in the center of mass from 1966 to 22 eV/u, respectively. Also, for the $CO^+$ measurements, CO ($M = 29$) enriched with $^{13}C$ was used in the source to avoid contamination with any $N_2^+$ ($M = 28$) ions which may be present.

The D beam is obtained by photodetachment of a 9.1-keV $D^-$ beam as it crosses the optical cavity of a 1.06-$\mu$m, 100-W cw neodymium-doped yttrium aluminium garnet (Nd:YAG) laser, where kilowatts of continuous power circulate. The voltage cell labeled in Fig. 1 can be used to fine tune the velocity of the $D^-$ beam at meV/u center-of-mass collision energies. However, for these measurements at eV/u center-of-mass energies and above, the cell is not used and is grounded. The 9.1-keV $D^-$ beam is produced be a commercial duoplasmatron ion source with mass selection by a 30° bending magnet. After photodetachment, the surviving $D^-$ ions are removed from the neutral D beam using electrostatic deflection. The ion and neutral beams interact along a field-free merge path, after which the $D^+$ product ions are magnetically separated from the primary beams. An electrostatic deflector produces the final deflection out of the plane of magnetic dispersion (see Fig. 1). The product signal $D^+$ ions are detected with a channel electron multiplier (CEM) operated in a pulse counting mode. The beam-beam signal rate (Hz) is extracted from (kHz) backgrounds with a two-beam modulation technique. $D^+$ backgrounds come from D stripping on background gas in the merge path. The vacuum pressure in the merge path is kept at $\sim 4 \times 10^{-10}$ Torr with the beams.

The independently absolute cross section is calculated from directly measurable parameters including the $D^+$ product count rate, the measured overlap of the two beams, the velocities of the ion and neutral beams, and the beam intensities. The velocities of the beams are calculated from the acceleration potentials, including estimated plasma shifts in the ion sources (see, e.g., Ref. [11]). The overlap of the two beams is measured from profiles obtained using two mechanical slits (labeled as slit scanner M1 and M2 in Fig. 1) and one dual rotating wire scanner [16]. The neutral beam intensity is measured by using secondary electron emission from a stainless-steel plate; the secondary emission coefficient is calibrated *in situ* [17]. While merged-beam measurements typically can access meV/u to keV/u collision energy, the measurements here were limited. Our measurements for $CO^+$ and $O_2^+$ could not extend below 20 eV/u due to the requirement that the signal $D^+$ at 9.1 keV has to be deflected to

62.5° by a magnetic field which is not always strong enough to deflect the entire $O_2^+$ or $CO^+$ primary beam into the demerge Faraday cup. This is a problem for the higher molecular ion velocities needed to access lower center-of-mass collision energies.

Although the ECR source produces molecular ions by energetic electron impact in diffuse plasma, there is no direct coupling between the power injected into the source and the internal energies of the ions themselves. These molecular ions are produced with certain vibrational and rotational excitations. We know of no investigation of the electronic states of ECR-produced molecular ions. However, the distribution of the rovibrational states should be similar to the ones produced by conventional electron impact ion sources which have been observed to be determined by Frank-Condon transitions between the electronic ground states of $D_2$ and $D_2^+$, $O_2$ and $O_2^+$, and CO and $CO^+$ [18–23]. In addition to the electronic ground state $X\,^2\Sigma^+$, calculations [24] show that $CO^+$ excited states $A\,^2\Pi$ and $B\,^2\Sigma^+$ can also be formed by the electron impact. The excited state $CO^+(B\,^2\Sigma^+)$ with a measured lifetime of 45 ns [25,26] is not expected to survive the 5–15 $\mu$s time of flight to the merged-beam apparatus. However, some excited $CO^+$ $(A\,^2\Pi)$ with a measured lifetime of several microseconds [27] might be present during measurements. For $O_2^+$, van der Zande *et al.* [20] have observed the production of $O_2^+$ $(a\,^2\Pi_u)$ metastable in a conventional electron impact ion source, for which the electronic ground state is $O_2^+$ $(X\,^2\Pi_g)$. The amount of $CO^+$ $(A\,^2\Pi)$ or $O_2^+$ $(a\,^2\Pi_u)$ decreases with the electron impact energy and is not significant if the electron energy is below the required energy to ionize CO or $O_2$ to these electronically excited states.

## III. RESULTS AND DISCUSSION

Our results for $(CO^+,D)$ and $(O_2^+,D)$ are presented in Tables I and II, respectively, along with relative and absolute errors at a 90% confidence level [10]. Figure 2 shows our measurements for $CO^+$ and $O_2^+$ in comparison with our previous $D_2^+ + H$ measurements and various theories for $H_2^+ + H$ and $CO^+ + H$. Previous experimental and theoretical studies of CT with $O_2^+$ in the literature include Cs, $H_2$, and $O_2$ targets [20,28–30], but we know of no CT study for $O_2^+ + H$ or isotopic D. Preliminary measurements for $CO^+ + D$ were reported in conference proceedings [9].

While the $Q$ value of the $O_2^+ + D$ endoergic reaction is $-1.5$ eV, the $Q$ values for the exoergic reactions $D_2^+ + H$ and $CO^+ + D$ are 2.0 and 0.4 eV, respectively, for $v = v' = 0$ [4,18,20,31–34]. At keV/u energies, the collision can be considered rovibrationally frozen and the differences in the $Q$ values are not a factor as all three cross sections converge to $(7.5 \pm 0.5) \times 10^{-16}$ cm$^2$ at 2 keV/u and are consistent

TABLE I. Measured charge transfer cross sections for $CO^+ + D$. Relative and statistical errors are listed below and correspond to a 90% confidence level.

| Energy (eV/u) | Cross section ($10^{-16}$ cm$^2$) | Relative error ($10^{-16}$ cm$^2$) | Absolute error ($10^{-16}$ cm$^2$) |
|---|---|---|---|
| 19.8 | 2.0 | 0.2 | 0.3 |
| 30.7 | 2.5 | 0.3 | 0.4 |
| 41.3 | 4.1 | 0.4 | 0.6 |
| 48.5 | 5.2 | 0.3 | 0.7 |
| 70.7 | 5.7 | 0.5 | 0.9 |
| 98.0 | 5.9 | 0.3 | 0.8 |
| 131 | 6.5 | 0.3 | 0.9 |
| 169 | 6.7 | 0.5 | 1.0 |
| 213 | 6.9 | 0.4 | 0.9 |
| 324 | 6.7 | 0.3 | 1.0 |
| 459 | 6.9 | 0.3 | 0.9 |
| 657 | 7.5 | 0.4 | 1.0 |
| 900 | 8.0 | 0.4 | 1.0 |
| 1224 | 7.8 | 0.4 | 1.0 |
| 1672 | 7.7 | 0.4 | 1.0 |
| 1923 | 7.9 | 0.4 | 1.0 |

TABLE II. Measured charge transfer cross sections for $O_2^+ + D$. Relative and statistical errors are listed below and correspond to a 90% confidence level.

| Energy (eV/u) | Cross section ($10^{-16}$ cm$^2$) | Relative error ($10^{-16}$ cm$^2$) | Absolute error ($10^{-16}$ cm$^2$) |
|---|---|---|---|
| 21.7 | 6.9 | 0.5 | 1.0 |
| 29.4 | 6.3 | 0.4 | 0.9 |
| 35.1 | 7.1 | 0.4 | 1.0 |
| 52.0 | 5.2 | 0.4 | 0.7 |
| 72.8 | 5.2 | 0.5 | 0.8 |
| 97.0 | 6.8 | 0.6 | 1.0 |
| 127 | 6.4 | 0.4 | 0.9 |
| 199 | 7.5 | 0.5 | 1.0 |
| 328 | 7.7 | 0.5 | 1.1 |
| 473 | 8.2 | 0.4 | 1.1 |
| 567 | 8.0 | 0.4 | 1.0 |
| 761 | 7.4 | 0.4 | 1.0 |
| 986 | 7.3 | 0.5 | 1.0 |
| 1385 | 7.3 | 0.5 | 1.0 |

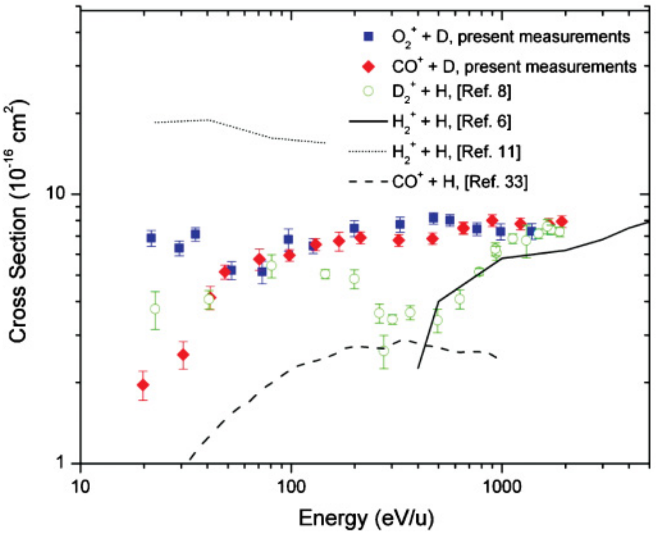

FIG. 2. (Color online) ORNL ion-atom merged-beam cross sections for $(O_2^+,D)$, $(CO^+,D)$, and $(D_2^+,H)$ compared to theory for $(H_2^+,H)$ by Errea *et al.* [6] and by Krstic [11] and for $(CO^+,H)$ by Lin *et al.* [32].

TABLE III. The collision time is shown as a function of collision energy and can be compared to the characteristic vibrational time of 50 a.u. (see text for details).

| Collision energy | 20 eV/u | 100 eV/u | 400 eV/u | 2000 eV/u |
|---|---|---|---|---|
| Collision time | 20 a.u. | 10 a.u. | 5 a.u. | 2 a.u. |

with the $H_2^+ + H$ calculations [6] at keV/u energies (see Fig. 2). The discrepancy of the $CO^+ + D$ measurements with the $CO^+ + H$ state-to-state calculations with Lin *et al.* [32] is not understood. The calculations shown here are for an angle-averaged 300-K Boltzmann distribution of the initial vibrational states. A more detailed discussion is found in Ref. [9].

As seen in Fig. 2, below 2 keV/u the cross sections for $O_2^+$ and $CO^+$ are relatively flat while the $D_2^+$ measurements and $H_2^+$ theory decrease. Vibrational times of the molecular ions can be compared to collision times to assess the possible role of vibrational states. The energy of the excited vibrational level with respect to the ground vibrational level determines the characteristic vibrational time of the molecular ions. The first vibrational states in $O_2^+$, $CO^+$, and $D_2^+$ are comparable and correspond to 0.23, 0.25, and 0.19 eV, respectively [18–20,32,34]. An average vibrational energy level of 0.5 eV corresponds t ∼ 50 a.u. in time. This vibration time can be compared to the various collision times calculated for our range of collision energy and assuming an interaction length of 1 a.u. From Table III we note that the typical vibrational time of 50 a.u. is significantly longer than the collision times at and above 100 eV/u, and therefore it seems reasonable that the collision can be considered frozen in this energy range. Indeed, a theoretical study by Lin *et al.* [32] indicates that, for ($CO^+$,H), the collision can be considered frozen down to 100 eV/u. In addition, the measurements for $D_2^+$ agree with the $H_2^+$ calculations, which are based on a sudden approximation (rovibrational modes frozen) and straight-line trajectories [6]. The fact that the collision can be considered vibrationally frozen above 100 eV/u suggests that the difference between the measured CT cross sections for $O_2^+$, $CO^+$, and $D_2^+$ is not due to dynamical vibrational states.

Relatively flat decreasing CT cross sections at collision energies below the CT maximum have been previously observed for other systems. A flat cross section is consistent with an absorbing-sphere model [35] which assumes that there are sufficient crossings between the initial and final potential energy curves that CT can always occur. If favorable crossings are not present, then a decreasing cross section would occur until the "reaction" window moves to a favorable crossing. This Landau-Zener curve crossing picture is often used to understand CT with atomic ions, e.g., it is used to explain observed *Z* oscillations in CT with highly charged ions on H [36]. Figure 3 shows a variety of 4+ ions where the CT cross section with H (or D) was measured [37–40] with the ion-atom merged beams over an extended energy range. Note that the cross sections are similar at keV/u energies but can be different by approximately two orders of magnitude, depending on the number of electrons on the core. The cross sections for $Si^{4+}$ and $Ne^{4+}$ are generally larger than the $N^{4+}$ and $C^{4+}$ with fewer electrons on the core. While detailed molecular orbital close-coupling calculations exist for these systems, one may try to understand CT using a Landau-Zener curve-crossing model. The flat energy dependence for the ions with multielectron cores indicates an abundance of favorable crossings. The larger quantum defect for the $Ne^{4+}$ and $Si^{4+}$ ions leads to larger splittings between possible capture states. Larger splittings spread potential crossings over a wider range of internuclear separation.

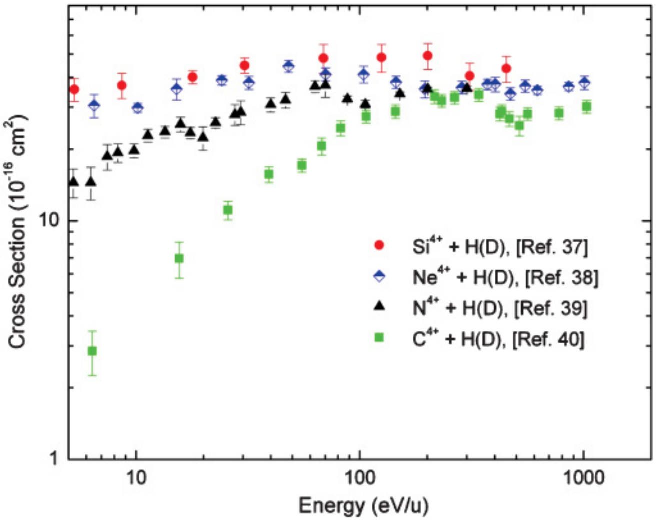

FIG. 3. (Color online) ORNL ion-atom merged-beam measurements for various $q = 4+$ ions with H(D) over an extended energy range.

Without the availability of detailed molecular potentials one might expect that the multielectron cores of $O_2^+$ and $CO^+$ would lead to more states for the complex $(O_2,D)^+$ and $(CO,D)^+$ than for $(H_3)^+$ and to an abundance of favorable crossings for charge transfer similar to the 4+ atomic ion cases. The resultant cross section is relatively flat compared to the $D_2^+ + H$ cross section which involves only two electrons (see Fig. 2).

While all three CT cross sections for diatomic molecular ions coincide at 100 eV/u, $O_2^+$ and $CO^+$ diverge below 60 eV/u with their different atomic cores. CT for $O_2^+$ remains relatively constant whereas CT for $CO^+$ decreases. At these energies we expect the rovibrational states to play an important part, as predicted by theory and through the collision times estimated in Table III. Detailed state-to-state molecular-orbital close-coupling calculations are required for reliable calculations. Toward lower energies, the $O_2^+$ cross section is expected to decrease due to the fact that the reaction is endoergic by 1.5 eV. Such thresholds have been observed for ($D_3^+$,H) CT measurements [19] using the ORNL ion-atom merged beams.

## IV. CONCLUSION

Absolute CT cross sections during ($CO^+$,D) and ($O_2^+$,D) collisions were measured from 20 eV/u to 2 keV/u collision energy, using the merged-beam technique. A discrepancy is seen with $CO^+$ + H state-to-state and angle-averaged calculations of Lin *et al.* [32]. Results are compared with our previous measurements for $D_2^+ + H$ and theory for $H_2^+ + H$. Toward a higher collision energy, the CT cross sections all converge to $(7.5 \pm 0.5) \times 10^{-16}$ cm$^2$ at 2 keV/u. At lower energy, the flat energy dependence of the CT cross sections observed with the $CO^+$ and $O_2^+$ ions suggests a multitude of favorable crossings, an assumption inherent in the absorbing-sphere model and previously observed for CT with atomic ions with many electrons on the core. A relatively poor agreement with the sparse theory suggests more work is needed for understanding molecular ion-neutral reactions.

## ACKNOWLEDGMENTS

This research is supported by the Office of Fusion Energy Sciences and the Division of Chemical Sciences, Geosciences, and Biosciences, Office of Basic Energy Sciences of the US Department of Energy. V.M.A. is supported by the National Science Foundation through Grant No. PHY-1068877. I.N.D is supported by the NASA Solar & Heliospheric Physics Program NNH07ZDA001N and acknowledges support from the ORNL Postdoctoral Research Associates Program, administered jointly by the Oak Ridge Institute for Science and Education and Oak Ridge National Laboratory.

[1] P. S. Krstic and R. K. Janev, Phys. Rev. A **67**, 022708 (2003).
[2] J. Woodall, M. Agundez, A. J. Markwick-Kemper, and T. J. Millar, Astron. Astrophys. **466**, 1197 (2007).
[3] W. Federer, H. Villinger, F. Howorka, W. Lindinger, P. Tosi, D. Bassi, and E. Ferguson, Phys. Rev. Lett. **52**, 2084 (1984).
[4] P. S. Krstic, Phys. Rev. A **66**, 042717 (2002).
[5] P. S. Krstic, Controlled Fusion Atomic Data Center (Online), Oak Ridge National Laboratory [http://www-cfadc.phy.ornl.gov/h2mol/home.html] (1 October 2011).
[6] L. F. Errea, A. Macias, L. Méndez, I. Rabadán, and A. Riera, Nucl. Instrum. Methods Phys. Res., Sect. B **235**, 362 (2005).
[7] C. McGrath, M. B. Shah, P. C. E. McCartney, and J. W. McConkey, Phys. Rev. A **64**, 062712 (2001).
[8] V. M. Andrianarijaona, J. J. Rada, R. Rejoub, and C. C. Havener, J. Phys. Conf. Ser. **194**, 012043 (2009).
[9] C. C. Havener, I. N. Draganić, and V. M. Andrianarijaona, in *Proceedings of the Twenty-First International Conference on Application of Accelerators in Research and Industry*, edited by F. D. McDaniel and B. L. Doyle, AIP Conf. Proc. No. 1336 (AIP, Melville, NY, 2011), p. 101.
[10] C. C. Havener, M. S. Huq, H. F. Krause, P. A. Schulz, and R. A. Phaneuf, Phys. Rev. A **39**, 1725 (1989).
[11] C. C. Havener, in *Accelerator-Based Atomic Physics Techniques and Applications*, edited by S. M. Shafrooth and J. C. Austin (AIP, New York, 1997), p. 117.
[12] C. C. Havener, in *The Physics of Multiply and Highly Charged Ions*, edited by Fred J. Currel (Kluwer Academic, Norwell, MA, 2003), Vol. 2, p. 193.
[13] I. N. Draganic, D. G. Seely, and C. C. Havener, Phys. Rev. A **83**, 054701 (2011).
[14] I. N. Draganic, M. E. Bannister, F. W. Meyer, C. R. Vane, and C. C. Havener, Nucl. Instrum. Methods Phys. Res., Sect. A **640**, 1 (2011).
[15] C. C. Havener, E. Galutschek, R. Rejoub, and D. G. Seely, Nucl. Instrum. Methods Phys. Res., Sect. B **261**, 129 (2007).
[16] D. G. Seely, H. Bruhns, D. W. Savin, T. J. Kvale, E. Galutschek, H. Alibadi, and C. C. Havener, Nucl. Instrum. Methods Phys. Res., Sect. A **585**, 69 (2008).
[17] J. D. Thomas, T. J. Kvale, S. M. Z. Strasser, D. G. Seely, and C. C. Havener, in *Proceedings of the Twentieth International Conference on Application of Accelerators in Research and Industry*, edited by F. D. McDaniel and B. L. Doyle, AIP Conf. Proc. No. 1099 (AIP, Melville, NY, 2009), p. 154.
[18] F. von Busch and G. H. Dunn, Phys. Rev. A **5**, 1726 (1972).
[19] V. M. Andrianarijaona, Ph.D. thesis, Université Catholique de Louvain, 2002.
[20] W. J. van der Zande, W. Koot, J. R. Peterson, and J. Los, Chem. Phys. Lett. **140**, 175 (1987).
[21] A. Petrignani, F. Hellberg, R. D. Thomas, M. Larsson, P. C. Cosby, and W. J. van der Zande, J. Phys. Conf. Ser. **4**, 182 (2005).
[22] S. Laubé, L. Lehfaoui, B. R. Rowe, and J. B. A. Mitchell, J. Phys. B: At. Mol. Opt. Phys. **31**, 4181 (1998).
[23] S. Rosén, R. Peverall, M. Larsson, A. Le Padellec, J. Semaniak, Å. Larson, C. Strömholm, W. J. van der Zande, H. Danared, and G. H. Dunn, Phys. Rev. A **57**, 4462 (1998).
[24] J. F. M. Aarts and F. J. De Heer, Physica **49**, 425 (1970).
[25] J. Desesquelles, M. Dufay, and D. C. Poulizac, Phys. Lett. A **27**, 96 (1968).
[26] R. G. Bennett and E. W. Dalby, J. Chem. Phys. **32**, 1111 (1960).
[27] R. Anderson and M. Jursich, Am. J. Phys. **43**, 535 (1975).
[28] A. T. Hasan and T. J. Gray, Int. J. Mol. Sci. **8**, 1158 (2007).
[29] T. F. Moran, M. R. Flannery, and P. C. Cosby, J. Chem. Phys. **61**, 1261 (1974).
[30] A. V. Yevseyev, A. A. Radtsing, and B. M. Smirnov, J. Phys. B **15**, 4437 (1982).
[31] G. H. Dunn, Phys. Rev. **172**, 1 (1968).
[32] C. Y. Lin, P. C. Stancil, Y. Li, J. P. Gu, H. P. Liebermann, R. J. Buenker, and M. Kimura, Phys. Rev. A **76**, 012702 (2007).
[33] J. S. Morrill, M. L. Ginter, B. R. Lewis, and S. T. Gibson, J. Chem. Phys. **111**,173 (1999).
[34] P. H. Krupenie and S. Weissman, J. Chem. Phys. **43**, 1529 (1965).
[35] R. E. Olson and A. Salop, Phys. Rev. A **14**, 579 (1976).
[36] F. W. Meyer, A. M. Howald, C. C. Havener, and R. A. Phaneuf, Phys. Rev. Lett. **54**, 2663 (1985).
[37] Marc Pieksma, M. Gargaud, R. McCarroll, and C. C. Havener, Phys. Rev. A **54**, R13 (1996).
[38] C. C. Havener, R. Rejoub, C. R. Vane, H. F. Krause, D. W. Savin, M. Schnell, J. G. Wang, and P. C. Stancil, Phys. Rev. A **71**, 034702 (2005).
[39] L. Folkerts, M. A. Haque, C. C. Havener, N. Shimakura, and M. Kimura, Phys. Rev. A **51**, 3685 (1995).
[40] F. W. Bliek, R. Hoekstra, M. E. Bannister, and C. C. Havener, Phys. Rev. A **56**, 426 (1997).